Available online at www.sciencedirect.com
ScienceDirect
ELSEVIER
Palaeogeography, Palaeoclimatology, Palaeoecology 239 (2006) 334–354
PALAEO
www.elsevier.com/locate/palaeo

Centennial to millennial changes in maar-lake deposition during the last 45,000 years in tropical Southern Africa (Lake Masoko, Tanzania)

Yannick Garcin [a,*], David Williamson [a], Maurice Taieb [a], Annie Vincens [a], Pierre-Etienne Mathé [a], Amos Majule [b]

[a] *CEREGE, UMR 6635, Université Aix-Marseille III, BP 80, 13545 Aix-en-Provence cedex 04, France*
[b] *Institute of Resource Assessment, University of Dar-es-Salaam, P.O. Box 35 097, Tanzania*

Received 5 September 2005; received in revised form 12 January 2006; accepted 12 February 2006

Abstract

The Masoko maar (southern Tanzania) provides one of the most continuous Late Quaternary lacustrine sedimentary records from Africa. A detailed chronostratigraphic framework coupled with sedimentological and magnetic measurements allows us to construct a 30-year resolution continuous sedimentary sequence covering the last 45,000 years and to address local depositional environment and climate variability in the tropical Southern Africa. Based on present-day observations and measurements, our results indicate that the low-field magnetic susceptibility of the sediment is highly controlled by climate-driven processes (wind-stress and/or lake-level amplitude changes) acting on the titanomagnetite-rich shoreline reservoir. The tephra- and turbidite-free magnetic susceptibility record is strongly modulated by a persistent multi-decadal to centennial variability (~80 to 200 years), probably linked to the Gleissberg and Suess cycles of solar activity. At lower frequency, the variability of deposition is controlled by the precessional cycle and its harmonics, suggesting a dominant multi-millennial forcing of low-latitude insolation on climatic changes in tropical Southern Africa. Inferred wetter conditions during the Last Glacial Maximum and the Younger Dryas at Masoko (9°S) indicate southward shifts of the Intertropical Convergence Zone associated with the North Atlantic glacial dynamics, and/or contrasted hydrological changes in the Rungwe highlands compared to the neighbouring areas. Finally, former regional transfer function between diatom assemblages and water chemistry suggested drier conditions during the Last Glacial Maximum at Lake Masoko [Barker, P., Williamson, D., Gasse, F., Gibert, E., 2003. Climatic and volcanic forcing revealed in a 50,000-year diatom record from Lake Massoko, Tanzania. Quaternary Research 60, 368–376]. In this context, further climate-proxy data (such as pollen) and hydrobiological studies in small, deep lakes are needed to support our alternative interpretation of the Masoko record.

Keywords: Lake Masoko; Rungwe; Southern Africa; Late Quaternary; Intertropical Convergence Zone; Precession; Solar cycles; Magnetic susceptibility

1. Introduction

Over the last decade, the recovery of numerous high-resolution paleoclimate records from ice, ocean sediments, speleothems or lake sediments has highlighted

* Corresponding author. Fax: +33 04 42 97 15 95.
E-mail address: garcin@cerege.fr (Y. Garcin).

0031-0182/$ - see front matter © 2006 Elsevier B.V. All rights reserved.
doi:10.1016/j.palaeo.2006.02.002

the centennial to millennial variability of the global climate during the Last Glacial Period [GRIP and GISP2 ice cores (Grootes et al., 1993); Cariaco basin (Peterson et al., 2000); Hulu cave (Wang et al., 2001)]. At local and regional scale, however, the number of continuous and detailed proxy-records covering both the Last Glacial and Holocene time intervals is still insufficient for the observation of the persistence and the relative control of climate oscillatory modes on terrestrial ecosystems (Rahmstorf, 2003; Schulz et al., 2004). This is especially the case in Africa, where contrasted hydrological changes in numerous depositional environments did not favour continuous deposition since the Last Glacial, even in large regional lakes (Street and Grove, 1979; Johnson et al., 1996; Gasse, 2000). To date in tropical Africa, only five small lakes [Lake Bosumtwi, Ghana (Talbot and Johannessen, 1992; Peck et al., 2004); Lake Barombi Mbo, Cameroon (Thouveny and Williamson, 1988; Maley and Brenac, 1998); Sacred Lake (Huang et al., 1999), Lake Rutundu (Ficken et al., 2002) and Lake Nkunga (Ficken et al., 1998) on Mount Kenya] and one regional great lake [lake Malawi (Johnson et al., 2002)] do provide continuous detailed records encompassing the Last Glacial Maximum [LGM; 23,000–19,000 calendar year before present (cal. year BP) (Mix et al., 2001)] and the Holocene until the present-day. As a result, the current chronostratigraphy of climatic/environmental changes and its associated data-model comparison approach (Pinot et al., 1999; Barker and Gasse, 2003) are broadly restricted to millennial time resolutions and regional scale at most (Mayewski et al., 2004), with a lack of data concerning lowland terrestrial ecosystems (<1000 m above sea level (a.s.l.)).

In this context, the Masoko maar lake (LM) in southern Tanzania provides one of the most detailed and continuous ~45,000-year-long terrestrial sedimentary sequence from Southern East Africa (Williamson et al., 1999; Gibert et al., 2002). Although previous studies of the Mackereth core MM-8 and Sedidrill core M96-A of LM have already yielded Late Quaternary records of vegetation and hydrological proxies (Barker et al., 2000; Barker et al., 2003; Thevenon et al., 2003; Vincens et al., 2003), no improved high resolution depositional record has yet been established from the whole set of available cores. Based on a detailed chronostratigraphical framework coupled with sedimentological and magnetic measurements, we present here the first high resolution (~30 years) sedimentary record of Lake Masoko across the last 45,000 cal. year BP. Our aim is (i) to characterize the main depositional patterns of LM maar deposition along an improved chronology, and (ii) to further address the local and regional environment and climate variability for this tropical region of Southern Africa.

2. Regional setting

Lake Masoko (9°20.0′S, 33°45.3′E, 840 m a.s.l.) is a maar-type volcanic crater from the Rungwe volcanic area, north of Lake Malawi and south of the Poroto range (Fig. 1C). The Rungwe area covers a surface of ~1500 km^2 and corresponds to the intersection between the NW–SE Rift Valley and a NE–SW transverse structure, the Usangu depression, which belongs to the Western Branch of the East Africa Rift. The Rungwe area is thus a relay zone that accommodates the south Rukwa and north Malawi (Karonga) rift basins (Ebinger et al., 1993; Delvaux and Khan, 1998). It contains two main volcanic centres, Mount Rungwe (2961 m) and Mount Kiejo (2175 m). The volcanics overlie the Precambrian basement and Permo-Triassic (Karoo Formation) to Neogene sediments. Rungwe volcanism and tectonic activity started in the late Miocene (~8 Myr ago) and remained active in the Holocene (Ebinger et al., 1993). The youngest eruption of the Kiejo volcano is recorded during the end of the 18th century (Harkin, 1960). Lake Masoko belongs to a chain of maar volcanoes located 12 km south of Mount Kiejo along the Mbaka fault (Fig. 1C).

According to the dating of its oldest sediments and nearby volcanics, the Masoko crater was formed subsequent to ca. 50,000 years ago (Gibert et al., 2002). The crater-lake is surrounded by a circular tuff-ring and presents a typical U-shaped topography/bathymetry, with steep slopes and a flat bottom (Fig. 1D). The lake has a surface of 0.36 km^2 with a comparatively small catchment area of 0.22 km^2 (Table 1). Lake Masoko is an oligotrophic freshwater closed lake, without surface outlet (diameter = 700 m; maximum depth = 38 m).

As for many phreatomagmatic crater lakes, the lake is supported by a shallow regional groundwater aquifer (Bergonzini et al., 2001), which flows to Lake Malawi. Rainfall and lake level measurements from 2001 to 2004 as well as observations by local people during the last 40 years indicate that the Lake Masoko level is sensitive to rainfall variability and fluctuates by 1–2 m at seasonal to interannual scale. Although the lake catchment corresponds today to the inner slopes of the crater (crater wall), the lake level rise is limited to the south by a sill located 6 m above the present lake level. This sill is at the southeastern end of a small (7 ha) and flat cultivated depression, connected to the lake catchment

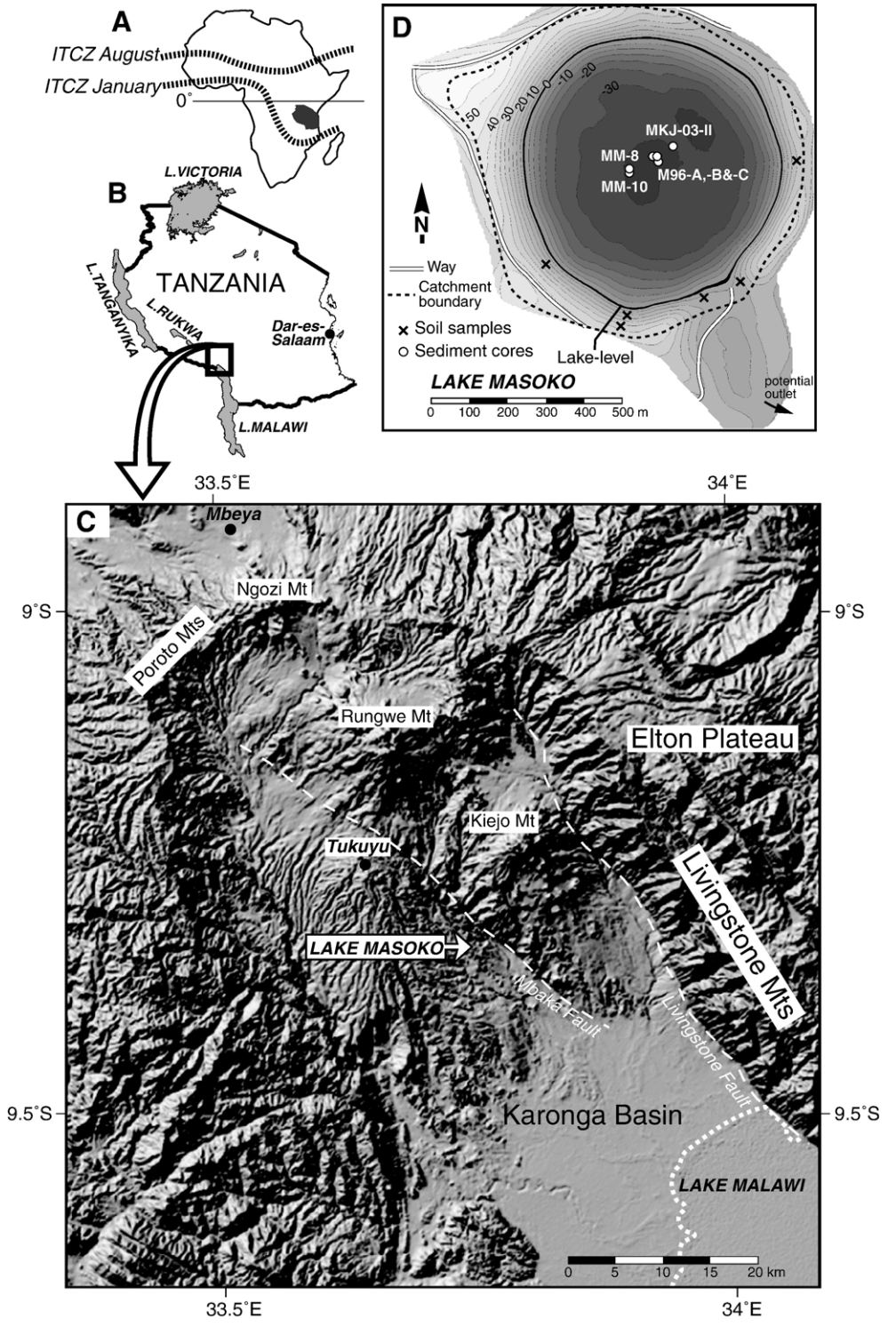

Fig. 1. (A) Present ITCZ seasonal migration over Africa (black dotted lines). (B) Location of the study area in Tanzania. (C) Rungwe volcanics shaded relief image (Shuttle Radar Topography Mission digital elevation model) showing the location of Lake Masoko. Also shown are the Ngozi, Rungwe and Kiejo volcanoes, the main faults and escarpments and the northernmost part of the Lake Malawi. (D) Lake Masoko relief map (isoline interval=5 m) with catchment area (dotted line), mean lake level, coring sites and soil sampling locations.

Table 1
Morphometric features and physical properties of Lake Masoko

Latitude/Longitude	9°20.0′S/33°45.3′E
Mean lake elevation	840 m a.s.l.
Annual lake-level variation	1–2 m
Maximum depth (average)	38 m
Mean depth (average)	13 m
Water volume	8.9×10^6 m^3
Lake surface area (L)	0.36 km^2
Catchment area (C)	0.22 km^2
Z-ratio (L/C)	1.6
Relative relief above mean lake elevation	60 m
Lake temperature (average)	28–30 °C
Lake conductivity	30–40 μS cm^{-1}
Lake pH	6.7–8

Data were obtained during field surveys in 1994, 1996, 2001, 2003 and 2004.

and possibly originating from a paleo-valley or -volcanic structure (Fig. 1D). Except from the top-rim and the shoreline area (see below), the inner slopes of the crater are short (50–70 m length) and steep (30° to 50°). The parent tuff-ring material outcrops in the steeper slopes (~50°) of the crater wall, where the sparse distribution of trees prevents any significant development or preservation of soils. It consists of unconsolidated volcanoclastics containing a mixture of weathered pumice, palagonitised tuff, and basalt or phonolite boulders. The coarser (sand- to meter-sized) erosion products of the tuff-ring concentrate in the shoreline area, where seasonal changes in lake level tend to remove the finer material by wave action. The outcome of such processes is the formation of a shoreline terrace, which provides the major reservoir for sand coarser material before transportation to the deep lake. The sublacustrine slope mostly consists of hard basaltic material, which outcrops between ca. 5 and 20 m below the present-day mean lake level. The bottom of this outcrop precisely corresponds to the depth of the lake thermocline (Merdaci, 1998). Soft sediments are found below this depth.

The catchment is forested and occupied by young ash soils. The thicker soil (1–2 m) develops on the relatively flat top rim area. In contrast, thinner soils (<20 cm) are observed in the inner slopes of the crater, where transportation processes dominate.

The vegetation of the low altitude Masoko area corresponds to a Zambezian "Miombo" woodland, and Afromontane formations occupy the surrounding highlands (White, 1983). Except for the top rim area where deforestation and cultivation occurred in a recent past, the catchment is occupied by dense *Brachystegia/Uapaca* woodlands (Vincens et al., 2003).

Regional climate is controlled by the seasonal variability of the intertropical convergence zone (ITCZ), which brings rains during one single season corresponding to the austral summer (from November to April), when the ITCZ is located in its southern position (Fig. 1A). The dry and windy season occurs from May to October (Nicholson, 1986; Nicholson and Yin, 2002). Locally, the climate of the southern Rungwe area (including Tukuyu and the Mbaka river valley) is significantly wetter than the average regional climate. The mean annual rainfall at Tukuyu (15 km north of Lake Masoko) is about 2400 mm year^{-1}, with monthly precipitation above 100 mm month^{-1} during the rainy season (Fig. 2) and a mean monthly temperature of 25 ±2 °C. Preliminary rainfall measurements at Lake Masoko since 2001 indicate similar high rainfall values, which contrast with the regional mean annual rainfall (~1200 mm year^{-1}) (Fig. 2). The high rainfall values of the Masoko and Tukuyu areas result from specific orographic features: evaporation of Lake Malawi to the south overloads the ascending air masses with humidity, while the high ranges to the north (Rungwe and Poroto) and east (Livingstone escarpment) (Fig. 1C) favour cloud condensation and rainfall (Bergonzini et al., 2001). A consequence of this setting is that the rainy season at Masoko extends until May, when trade winds strengthen in the Southern Hemisphere (Bergonzini et al., 2001). The result of these peculiar geographic, morphological and climatological settings is that, in contrast to most low-altitude lakes of intertropical Africa, Lake Masoko has not dried out since its formation (Bergonzini et al., 2001; Gibert et al., 2002; Barker et al., 2003). Due to the small size of the

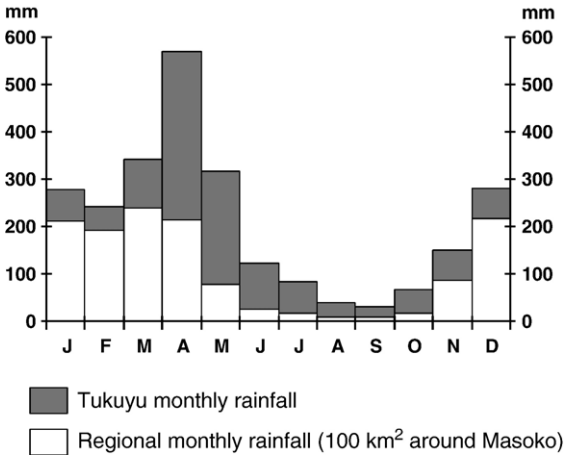

Fig. 2. Tukuyu and regional mean monthly rainfall histograms (mm month^{-1}). The latter is estimated on a 100×100 km area centred on Masoko (Climate Research Unit data sets; New et al., 2002).

catchment and to the oligotrophic freshwater environment, the mean apparent deposition rate in Lake Masoko was relatively low (less than 1 mm $year^{-1}$) over the last tens of millennia. Previous rock-magnetic (Williamson et al., 1999) and organic matter studies (Merdaci, 1998) indicated contrasting terrigenous inputs into the lake, with increased contributions of the poorly organic tuff-ring material during glacial times, and increased contributions of organic-rich soil components during the Holocene.

3. Material and methods

Fifteen sediment cores were retrieved in the deepest lake area since 1994 (Fig. 1D). Taken together, these cores overlap the entire depositional record in the lake since the formation of the crater, ca. 50,000 years ago (Williamson et al., 1999; Gibert et al., 2002; Barker et al., 2003). This study focuses on two 3-m-long Mackereth cores (MM-8 and MM-10), three 30-m-long sedidrill-Mazier cable cores (M96-A, -B and -C), and a 50-cm-long Kajak core taken from the subsurface sediments (MKJ-03-II). The stratigraphy and the correlation of the cores (vertical accuracy <1 cm) was based on sedimentary features (e.g., laminated intervals, turbidites, organic-rich layers, tephras) and on the measurement of water content, dry bulk density and magnetic susceptibility. This procedure allowed us to combine the most continuous cored sections and to construct a detailed 32-m-long composite lithostratigraphic record.

High resolution subsampling was performed at ~1-cm depth interval along the vertical core axis by using a 1-mL modified syringe. Dry bulk density, water content and low-field magnetic susceptibility were then measured on the whole set of samples (n=2383). Additional measurements (magnetic hysteresis) were carried on a set of pilot samples representative of the general stratigraphy and sediment sources.

The dry bulk density (DBD, g cm^{-3}) was calculated as the dry mass of the sample divided by its initial bulk (wet) volume (Avnimelech et al., 2001). The water content (%) was calculated as the mass of water to the total wet mass. Despite the sensitivity of DBD and water content to compaction effects, gas concentration and water evaporation during core transportation and storage, the combination of these parameters was useful to identify the major changes in lithology. Indeed, the DBD of relatively coarse inorganic sediments (e.g., pumice layers, some turbidites) is relatively high compared to organic-rich sediments, while the water content depends more especially on the sediment porosity, with higher values in organic-rich sediments. These sedimentological proxies were further compared to an estimation of the inorganic terrigenous component (ITC%) as calculated from total organic carbon (TOC) and biogenic silica (BSi) dry weight percentage data sets (Merdaci, 1998):

$$\mathrm{ITC}_{\mathrm{dryweight\%}} = 100 - (2.5 \times \mathrm{TOC}_{\mathrm{dryweight\%}}) - \mathrm{BSi}_{\mathrm{dryweight\%}}$$

Magnetic measurements were carried out on wet samples. The low-field magnetic susceptibility (χ_{lf}) was measured on a Kappabridge (KLY-2) and normalized to the dry mass of the sample. In addition to routine χ_{lf} measurements and existing rock-magnetic data (Williamson et al., 1999), rock magnetic measurements were performed on a set of samples considered as representative of the main sediment sources and depositional environments. This set included 40 soil samples taken from a series of soil profiles located along the catchment toposequence, from the top rim to the bottom slope of the crater wall (Fig. 1D). Measurements of the field dependence of AC magnetic susceptibility were performed on a Lakeshore model 7130 AC susceptometer at the Institute for Rock Magnetism of the University of Minnesota. The field dependence of AC susceptibility was measured at nine fields ranging from 30 to 2000 A m^{-1} (operating frequency: 40 Hz). The magnitude of the field dependence ($\chi_{ACD\%}$) was quantified by the percentage increase of susceptibility between 30 and 1000 A m^{-1}:

$$\chi_{\mathrm{ACD\%}} = 100(\chi 1000_{\mathrm{A\ m^{-1}}} - \chi 30_{\mathrm{A\ m^{-1}}})/\chi 30_{\mathrm{A\ m^{-1}}}.$$

Magnetic hysteresis loop measurements were performed on a micro-mag vibrating sample magnetometer (μVSM, Princeton Measurements) on 146 samples of lake-sediments, and on 40 samples of soils, tuff, rocks and littoral sands from the catchment (maximum field: 1 T, measurement time: 0.5 s, pause after removal of the applied field for remanence measurements: 1 s). The saturation magnetization (M_s), saturation remanent magnetization (M_{rs}) and coercive force (H_c) were calculated after correcting for the high-field slope (χ_{hf}) of the M–H curve (between 0.7 and 1 T). The coercivity of remanence (H_{cr}) was calculated from the backfield remanence curve. To further highlight the magnetic concentration changes in the lake catchment, a magnetic susceptibility surface mapping was made on two representative plots using a SM30 susceptometer (ZH instruments).

4. Core recovery and lithology

The general recovery of the 32-m-long LM cored sequence reaches 85%. Field observations showed that the 15% remaining lost material mostly consisted of unconsolidated coarse (sand- to gravel grain-sized) and hard pumice layers. The LM lithostratigraphy and its sedimentological record are shown in Fig. 3 and synthetic data are listed in Table 2. Four main lithozones are defined.

Lithozone I [from 32.5 to 29.3 m below the lake floor (b.l.f.)] consists in a ~3 m thick sequence of fine-grained lapillis and coarse degraded pumices in an olive yellow matrix including millimetric reddish kaolinized nodules. Organic and inorganic carbon is absent (Merdaci, 1998). The water content values are the lowest of the entire cored sequence (28% to 35%), while χ_{lf} and DBD values are the highest (1.5×10^{-5} to 5×10^{-5} m^3 kg^{-1} and 1 to 1.5 g cm^{-3}, respectively). This lithozone corresponds to weathered volcanic tuff and represents the bedrock of the lake.

Lithozones II to IV consist in the alternation of three main facies related to lacustrine sedimentation: organic silty muds, turbidites and tephras (Table 2).

The organic silty muds facies represent a cumulative thickness of 18.1 m (71.2% of the total recovered lacustrine sediments). These clayey to silty sediments are dark (black to olive) and highly porous (water content ~60%). DBD values in such facies are inversely correlated with water content. χ_{lf} values are relatively low (7.2×10^{-6} m^3 kg^{-1}) but highly variable (standard deviation ~3.9×10^{-6} m^3 kg^{-1}). Organic carbon content values range between 1% and 20%, with a 6.4% average while inorganic carbon is absent. The C/N ratio ranges between 10 and 35 with an average of ~24, pointing to the enrichment of organic material in terrestrial components (Merdaci, 1998). Fine laminations (<1 mm) are present in some intervals but could not be clearly associated with annual varves due to their irregular occurrence. Binocular and transmitted light microscope observations indicate that the organic silty mud facies is composed of: catchment-derived minerogenic material (rounded tuff grain, automorphous pyroxenes, feldspars and titanomagnetite), terrestrial plant remains, charcoals, phytoliths, pollen, amorphous organic matter, diatoms and occasionally authigenic vivianite concretions. Although the present-day lake bottom interface sediments are mixed over the upper centimeter, the remarkable preservation of organic remains in such sediments as well as the absence of bioturbation traces over the whole cored sequence point to a continuous, undisturbed deposition of suspended material from the water column to a suboxic lake bottom. The organic silty muds, which represent the background lithology, are also likely constrained by seasonal to decadal event-like terrigenous deposition. However, due to particle mixing at the sediment–water interface and/or to relatively low terrigenous inputs, it is not possible to firmly identify single "events" in this facies.

Sixty-four "macro-" turbidite layers (i.e., visible to the naked eye) have been defined along the sequence. They represent a cumulative thickness of 2.1 m (8.3% of the total recovered lacustrine sediments). Each turbidite consists of a single, light, brown to gray layer (from few millimetres to 36 cm thick), in which the bottom is defined by a sharp boundary, sometimes an erosive structure. Most turbidite layers show normal grading (fining upward), with a sandy to silty bottom and a clayey top. The sandy to silty layers show a χ_{lf} peak, characterizing an enrichment in (Ti-)magnetite particles. Turbidites are poorly organic (TOC <2%) and mostly contain clastic terrestrial material, including occasional plant remains and charcoal fragments. Compared to most organic silty muds, the turbidites show higher χ_{lf} and DBD values (~1.1×10^{-5} m^3 kg^{-1} and ~0.71 g cm^{-3}, respectively). As observed in many lake environments (Page et al., 1994; Eden and Page, 1998; Brown et al., 2002), the LM turbidite record indicates event-sedimentation processes likely triggered by climatic events or earthquake activity.

Finally, the LM sequence contains a record of tephra layers, which represents 20.5% of the recovered sediments. Seventy distinct tephra layers are observed. Moreover, some tephra layers have not been cored entirely, especially the coarsest and hardest pumice horizons, of which fragments were partly preserved at the extremity of the core gaps. The thickness of tephra layers range from some millimeters to 1.5 m. Most of these layers are characterized by a very light colour, from white, to pale yellow, light gray or pale olive. Tephra grain size ranges from fine ash to coarse lapilli. They are generally well bedded and well sorted. Fine ash beds show either normal or reverse grading while coarse pumice beds only show a normal grading. As for turbidites, tephra layers generally show relatively high DBD values (average 0.82 g cm^{-3}). Most of them are composed of low-χ_{lf} minerogenic material (χ_{lf} ~2.7×10^{-6} m^3 kg^{-1}), indicating poor contributions of ferromagnesian minerals and high contribution of diamagnetic glass shards and glassy sanidine monocrystals. Still, eight dark tephra layers containing obsidian-type glass shards enriched in magnetite show strong magnetic

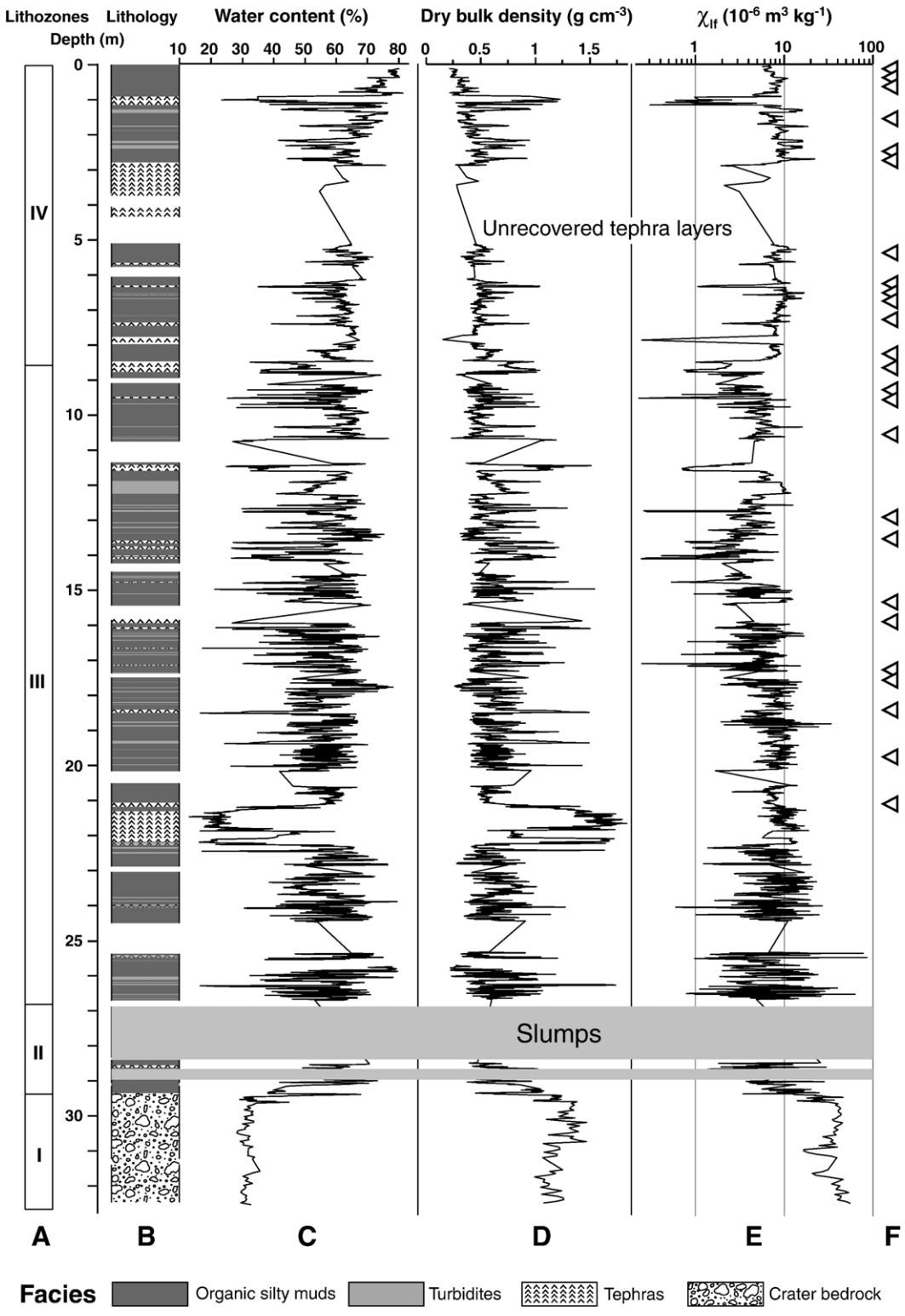

Fig. 3. Lake Masoko stratigraphic framework. The Masoko core (~32 m thick) is a combination of the most continuous cored sections. (A) Lithozones. (B) Lithology: stratigraphic distribution of the main facies. (C) Water content. (D) Dry bulk density. (E) Low-field magnetic susceptibility (χ_{lf}). Core gaps are the location of the unrecovered tephra layers (coarse sands and hard pumices destroyed by the rotative drilling). (F) Triangles are AMS radiocarbon ages (Gibert et al., 2002).

Table 2
Properties of the main lithological facies in the Lake Masoko record

Facies	Sample number	Water content (%)			Dry bulk density (g cm^{-3})			χ_{lf} (10^{-6} m^3 kg^{-1})		
		Mean	S.D.	Range	Mean	S.D.	Range	Mean	S.D.	Range
Organic silty muds	1843	60	10	24–81	0.54	0.19	0.22–1.73	7.2	3.9	1–86
Turbidites	255	52	8	17–74	0.71	0.20	0.45–1.93	11.0	7.0	1–78
Tephras (light)	207	46	12	17–78	0.82	0.26	0.23–1.50	2.7	2.3	0.2–11
Tephras (dark)	78	25	8	13–63	1.47	0.27	0.48–1.84	10.0	2.9	3–17

susceptibility values (average 1×10^{-5} m^3 kg^{-1}), especially an 80-cm-thick layer located at 22 m (Fig. 3). The Lake Masoko tephras are silicic and show a trachytic to phonolitic composition. They correspond to ash fall deposits that have recorded the past eruptive activity of the Rungwe Volcanic Centre (most especially the Rungwe, Kiejo and Ngozi volcanoes) (Harkin, 1960; Ebinger et al., 1989; Williams et al., 1993).

Lithozone II, from 29.3 m to about 26.8 m, corresponds to a basal, disturbed interval of slumped sediments, where numerous folds with a horizontal axis and a decimetric thickness are found. Due to the inability to reconstruct a detailed stratigraphy in this zone, these basal slumps have not been sampled systematically. Considering the absence of such slumps in the overlying Lithozones III and IV, the basal Lithozone II likely indicates a period of instability of the crater inner slopes during the initial stages of lacustrine deposition.

Lithozones III (from 26.8 to 8.7 m) and IV (from 8.7 m to the top) present the same general lithologic and sedimentary features. In contrast, the upper Lithozone IV shows less stratification and more organic sediments. The upward increase in water content and the associated decrease in DBD to the top of the sequence are caused by the lower compaction of the upper sediments.

5. Depth–age model

The chronology of the ~30 m long Lake Masoko sequence is based on a series of 25 AMS radiocarbon dates of organic matter or organic macrorests (charcoal, plant debris), calibrated for the changes in atmospheric ^{14}C (Gibert et al., 2002). The previous linear depth–age model (Barker et al., 2003) of cores MM-8 and M96-A and -B provided a general chronology down to ~45,000 cal. year BP. However, the occurrence of event layers such as slumps, turbidites, pumice-gravels and tephra horizons considerably restricted the reliability of this chronology between two successive dated horizons. Indeed, such layers are typically deposited over a period of some hours to some days, representing instantaneous events compared to the background sedimentation (Wilmshurst et al., 1997; Brown et al., 2002). Based on millimeter-scale observations and measurements in cores MM-10, M96-A, -B, and -C, which provided an updated set of correlations and a more detailed sequence stratigraphy, each tephra and turbidite layer thicker than ~1 mm was removed from the original depth scale. In addition, each coring "gap" that resulted from the destruction and loss of pumice layers during the drilling was also systematically removed. Finally, the

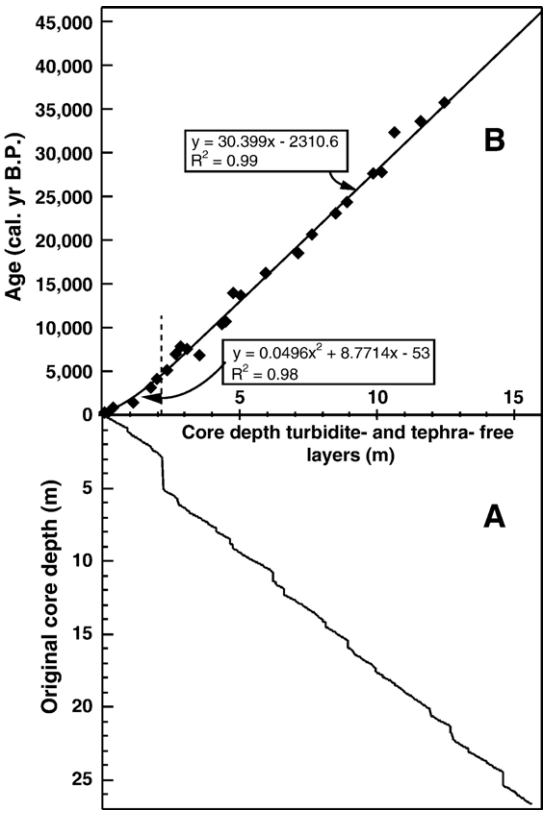

Fig. 4. (A) Relationship between the original composite core depth and the modified depth turbidite- and tephra-free layers. (B) Depth–age model of the LM sequence based on the turbidite- and tephra-free layers depth scale. A second order polynomial fit was established from the top to 208 cm and a linear fit from 208 cm to the bottom.

non-lacustrine crater bedrock sediments (Lithozone I) and the overlying slumps (Lithozone II) from the bottom of the sequence were also removed. The removal of all these event duration or non-lacustrine deposits yields a turbidite- and tephra-free depth scale, which is 14.5 m shorter (i.e., 48%) than the initial depth scale (Fig. 4A).

The calibrated radiocarbon ages (Gibert et al., 2002) were then assigned to the depth turbidite- and tephra-free layers (Fig. 4B). Using this set of ages, the lacustrine deposition was estimated by a second-order polynomial fit from the top to 2.08 m, and by a linear fit from 2.08 m to the bottom. The resulting LM sediment record ranges from −50 cal. year BP (AD 2003) to 45,300 cal. year BP, with a mean apparent sedimentation rate of 0.33 mm year^{-1}, which remains almost constant through time except in the upper, non-compacted part of the cored sequence.

6. Titanomagnetite-rich littoral sands and the low-field magnetic susceptibility of Lake Masoko rocks

In contrast with numerous lake sediments where the low-field magnetic susceptibility (χ_{lf}) is strongly controlled by the dilution (or dissolution) of high-χ_{lf}, ferro- or para-magnetic components in diamagnetic material of biogenic or authigenic origin (e.g., vegetal organic matter, biogenic silica, calcium carbonate) (Thouveny et al., 1994), the magnetic susceptibility of the oligotrophic LM sediments is poorly constrained by biogenic and/or authigenic components (Williamson et al., 1999). Detailed rock magnetic analyses from the rocks, soils and sediments indicated that the sediment χ_{lf} was mostly controlled by the concentration of "soft" detrital titanomagnetite, which is found primarily in high-χ_{lf} soils developing in the forested areas of the crater and in high-χ_{lf} shoreline sands, where the titanomagnetite fraction concentrates. The major control of primary clastic sources on the LM χ_{lf} record was further supported by additional magnetic analyses carried out on samples taken respectively from characteristic soil profiles made on the flat top rim area, from inner slope tuff-ring material and from shoreline material.

As shown on Fig. 5A, the strong correlation between χ_{lf} and M_{rs} values indicates that the susceptibility of the whole set of samples is mostly controlled by the

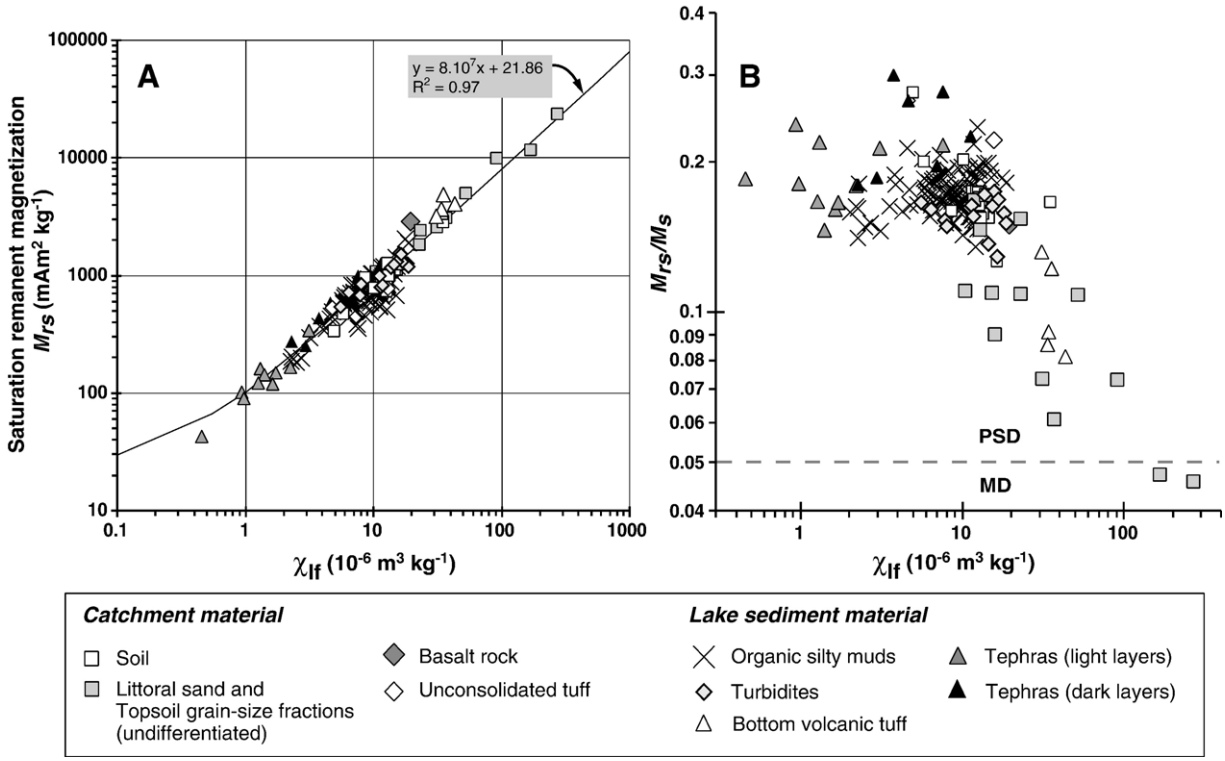

Fig. 5. Magnetic properties of the LM sediment and catchment material. (A) Binary χ_{lf}–M_{rs} diagram showing a linear relation. (B) Binary χ_{lf}–M_{rs}/M_s diagram showing the negative relationship between these two parameters [PSD=pseudo single domain, MD=multidomain (Day et al., 1977)]. Maximum susceptibility values correspond to the coarser magnetic grain-size component from pedogenized material and littoral sands.

ferrimagnetic fraction. The highest χ_{lf} value of soil or shoreline material (littoral sand) are associated with relatively low M_{rs}/M_s ratio values (Fig. 5B), indicating the dominant effect of coarse, multidomain (MD)-like spinels on the magnetic susceptibility. In addition to former low- and high-temperature experiments which indicate the occurrence of titanomagnetite in LM rocks (Williamson et al., 1999), additional measurements of the AC field dependence of magnetic susceptibility at room temperature show systematically positive $\chi_{ACD\%}$ values, pointing to irreversible domain-wall displacements in low fields, a characteristic behaviour of multidomain, Ti-rich magnetite (Jackson et al., 1998; de Wall, 2000) (Fig. 6). Not surprisingly, maximum $\chi_{ACD\%}$ values in soil and shoreline samples indicate a specific enrichment of these sediment sources in titanomagnetite.

Fieldwork observation and measurements such as soil hydraulic conductivity and erosion traps suggest that the input of the coarse (Ti-)magnetite in Lake Masoko is controlled by two main processes: (i) the transportation of the soil material to the littoral reservoir and (ii) the transportation of littoral material to the deep lake.

(i) Due to the high hydraulic conductivity (>1 m h^{-1}) of the young Lake Masoko ash soils (RESOLVE report, 2003; unpublished) and the highly porous tuff ring material of the catchment, surface runoff and rill erosion processes are almost absent on the crater slopes. Such peculiar properties of the catchment almost exclusively restrict erosional processes to "rain splash" processes. The latter are ineffective in transporting soil material, most especially the coarser and denser fraction, to the littoral lake area under present-day rainfall conditions. However, field observations also indicate a progressive mass transportation of the soil cover triggered by gravity (creeping) through the crater slopes to the littoral area, which may further explain the low ($\sim$0.33 mm year^{-1}) and relatively stable average apparent sedimentation rate into the lake during the last 45,000 years.

(ii) The littoral area possesses the highest χ_{lf} values of Lake Masoko rocks ($>5\times10^{-5}$ m^3 kg^{-1}) and is the major sand and heavy mineral reservoir of the basin (Fig. 7). Relatively high-energy conditions in this area naturally favour the preferential storage and sorting of dense and coarse material, enriched in multidomain (titano) magnetite, named the MDTM fraction. The transportation of the MDTM fraction to the deep lake environment is then controlled by the seasonal (and longer period) changes in lake level. Periods of relatively stable lake level and/or low wind-stress allow the accumulation of littoral sands and titanomagnetite-rich placers, which are found today along the littoral zone (Fig. 7) and in the upper 3 m of the water column. Such littoral sands are preferentially transported to the deep lake at the beginning of large amplitude (seasonal to longer period) changes in lake level, which are associated with a change in the wave action shore-zone (Pierce, 2004). Indeed, the dry and low-stand "winter" season is characterized by strong southeasterly tradewinds, which strengthen the action of waves on the lakeshore. According to such processes, any decrease in the amplitude of lake level changes combined with a shorter winter dry season would result in a stabilization of the littoral sand reservoir, and a preferential deposition of fine, low-χ_{lf} sediments into the deep lake. The most efficient MDTM sorting/storage process results in the lowest χ_{lf} values. Conversely, inefficient MDTM storage would favour a general increase in sediment χ_{lf}. This latter could be due to relatively steep shore slopes (e.g., in the early stages of the crater-lake deposition), exceptional rainfall, seismic events, or high amplitude lake level fluctuations combined

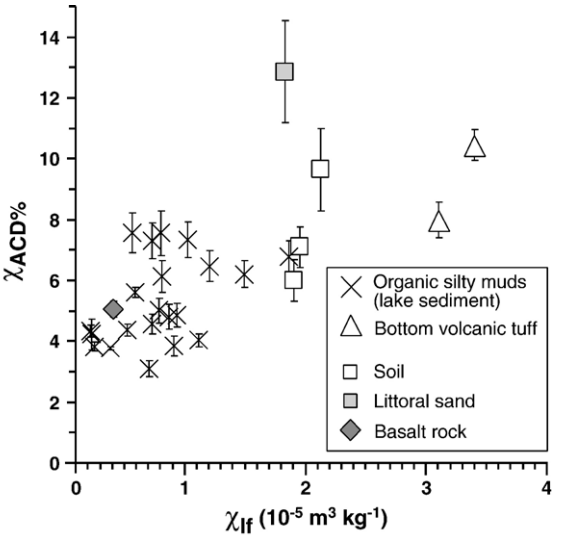

Fig. 6. Binary χ_{lf}–$\chi_{ACD\%}$ diagram for Lake Masoko sediment and catchment material showing the positive relationship between these two parameters. Maximum χ_{lf} and $\chi_{ACD\%}$ values correspond to the soil and the littoral sands indicating a titanomagnetite enhancement ($\chi_{ACD\%}$ error bars represent 1σ).

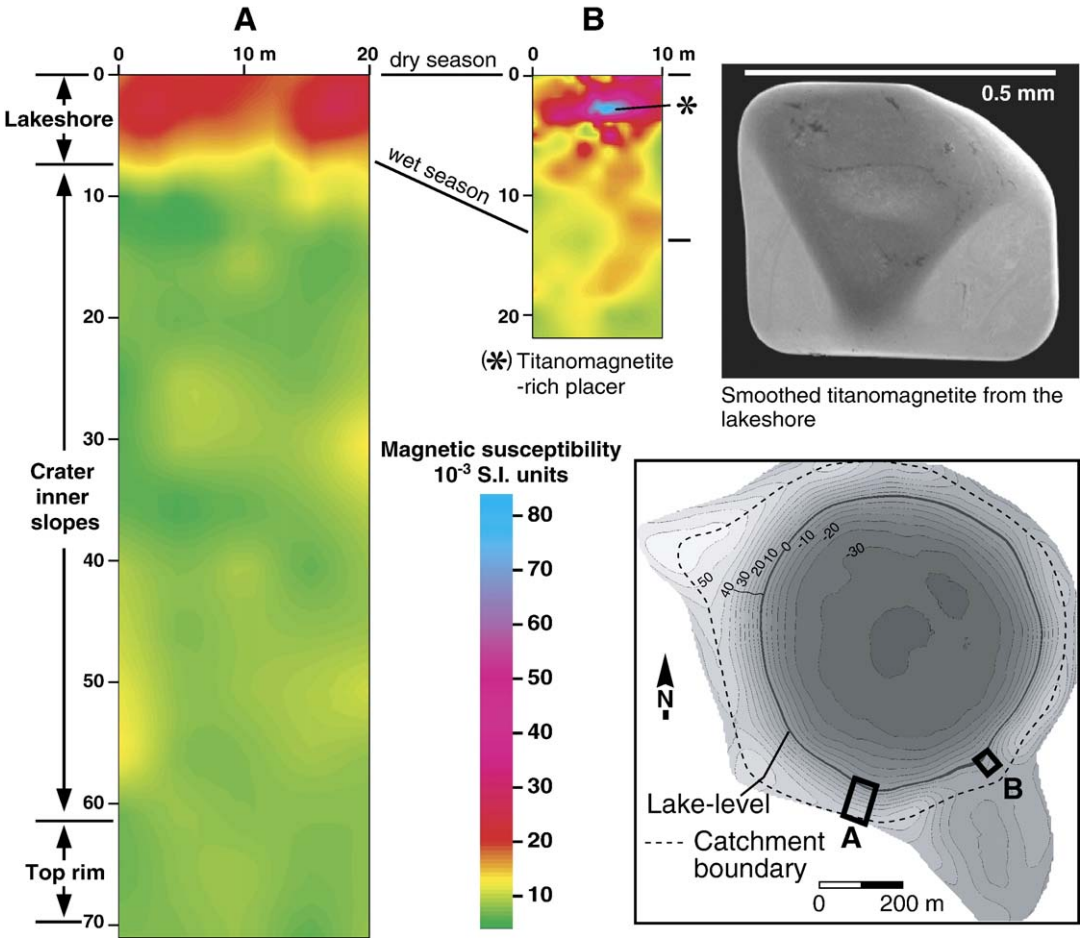

Fig. 7. Left: Magnetic susceptibility surface mapping of plots A and B on the Masoko catchment area. Note that the strong susceptibilities are on the lakeshore area. Bottom right: location map of plots A and B. Top right: SEM image of a smoothed titanomagnetite from the high-energy lakeshore area.

with drier conditions and strengthened wind-stress over the lakeshore.

7. General maar-lake deposition trends

Based on the above observations, the Lake Masoko χ_{lf} and DBD records provide insights on transportation and deposition processes in tropical maar lakes. In order to isolate the undisturbed sedimentation from volcanic deposits, seismites and other accumulations related to lake–slope instabilities, we have removed all the event layers from the record. The resulting turbidite- and tephra-free record then allows us to describe the general changes in depositional environment (Fig. 8).

The χ_{lf} record is first compared with the ITC% parameter, which reflects the general input in terrigenous material (Fig. 8A and B). Clearly, these two parameters are not correlated: the ITC% remains almost constant through time (average value), while the χ_{lf} record shows a low and high frequency variability exceeding an order of magnitude. These observations support earlier findings (Williamson et al., 1999) showing that the Masoko sediment χ_{lf} is poorly controlled by the dilution of ferrimagnetic particles in a para- or dia-magnetic matrix. They suggest that the sediment χ_{lf} reflects the relative contribution of the dominant MDTM source, rather than the general terrigenous component.

At the scale of the last 45,000 years, the absence of any significant drop in average magnetic susceptibility with time indicates that ash leaching and pedogenic processes, which result in the relative accumulation of MDTM in the catchment, are counterbalanced by the transportation of soil and littoral material to the lake. Such an observation is in agreement with several large-scale experiments, which indicate a close association

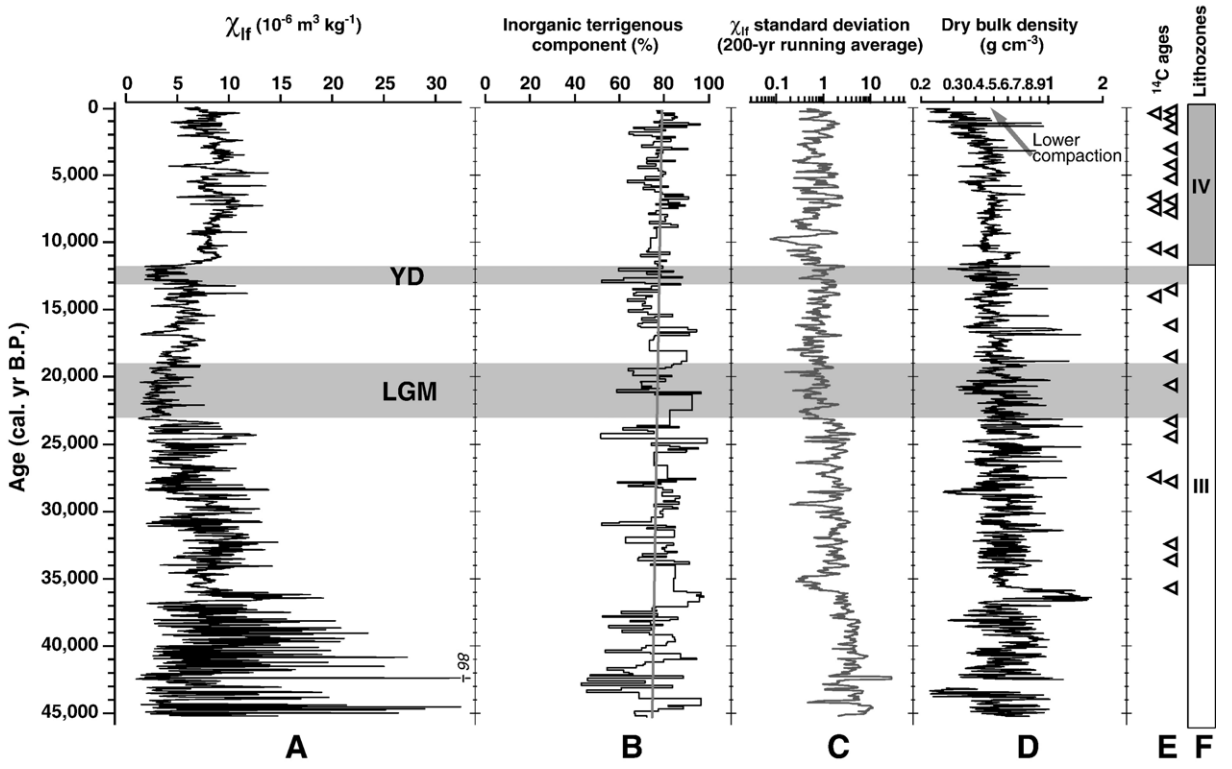

Fig. 8. Masoko paleoenvironmental data as function of age. (A) Magnetic susceptibility (χ_{lf} turbidite- and tephra-free layers). (B) Inorganic terrigenous component with its linear trend (gray line). (C) χ_{lf} standard deviation. (D) Dry bulk density. (E) AMS radiocarbon ages (Gibert et al., 2002). (F) Lithozones. The LGM and the YD intervals (black labels) are depicted by gray bands.

between chemical and mechanical erosion (Millot et al., 2002; Dupre et al., 2003).

The long-term evolution of the basin is also observed from the changes in amplitude of χ_{lf} oscillations. The upward decrease of respectively high frequency oscillations and χ_{lf} standard deviation values (Fig. 8A and C) indicates a progressive evolution of the crater catchment since its formation. This trend probably results from the weaker sensitivity of the crater slopes to erosional events, associated with long-term weathering processes and the smoothing of the lake catchment topography.

Despite this general trend, the low frequency oscillations of χ_{lf} or ITC% show lower amplitudes than the high frequency changes. This observation points to the dominant event-like nature of the lake deposition, which persists after the removal of the turbidite layers from the record. Given the relatively low mobility of the coarse MDTM fraction in the catchment (see Section 6), such strong and quick changes are probably driven by the sensitivity of the littoral sand reservoir, where titanomagnetite "placers" are found that present the maximum χ_{lf} values of Masoko-crater rocks (Fig. 7). A climatic control on the input of littoral MDTM sands primarily occurs through the seasonal to interannual amplitude change in lake level, wind-stress and/or the mean lake level. Both processes are associated with the average hydrological regime: wet conditions resulting in lake high-stands and/or shorter dry seasons favour the storage of the coarse heavy mineral fraction in the littoral area, while dry conditions favour the erosion of this reservoir and its transportation to the central and deep part of the lake through wave- and/or rain-action on a relatively low-stand shoreline. According to this conceptual model, large amplitude seasonal to interannual changes in lake level and/or relatively lake low-stands during dry periods would result in a χ_{lf} increase of the lake sediment. Low amplitude seasonal to interannual changes in lake level and/or relatively lake high-stands during wet periods would result in lower χ_{lf} values.

8. Depositional changes and lake-level oscillations across the last 45,000 years

Two major time intervals are shown by the turbidite- and tephra-free records of χ_{lf}, ITC% and DBD at Lake

Masoko. They respectively correspond to the Last Glacial Period (from 45,300 to 11,800 cal. year BP) where a strong variability of deposition is evidenced, and to the Holocene (from 11,700 cal. year BP to present-day time), where depositional changes show relatively lower amplitude (Fig. 8). Such contrasts primarily result from the dominant contribution of poorly weathered tuff and clastic material during the Last Glacial Period, progressively enriched in organic material during the Holocene. In addition to this general feature, however, the magnetic susceptibility record, owing to its dominant control by erosional processes in the shoreline area and lake-level oscillations, provides a more detailed observation.

From ~45,300 to 23,000 cal. year BP, relatively high but variable χ_{lf} values are observed. According to a probable control of lake level oscillations on the χ_{lf} record through littoral MDTM inputs, a general low-stand probably occurred during this period, most especially between 34,000 and 28,000 cal. year BP. The strong variability of deposition during the 45,000-36,000 cal. year BP time interval suggests that the lake-catchment system was very sensitive to any perturbation. Depositional processes were strongly controlled by seasonal to centennial climate variability. The progressive χ_{lf} decrease from ~31,000 until 23,000 cal. year BP likely indicates a transgressive trend and/or a stabilization of the lake level that favoured the trapping of the MDTM-rich sediment on the lakeshore.

From 23,000 to 19,000 cal. year BP, minimum χ_{lf} values indicate a low contribution of the MDTM source, suggesting that the lake level was stable or high enough to promote the storage of the coarser and heavy catchment material on the lakeshore area. This period corresponds precisely to the Last Glacial Maximum (Mix et al., 2001).

The 19,000–12,800 cal. year BP time interval encompasses the end of the LGM and the deglaciation (Morgan et al., 2002). During this interval, the χ_{lf} increases to reach a maximum at ~18,000 cal. year BP, suggesting a return to high-amplitude lake-level oscillations and/or a drop in the mean lake level.

From 12,800 to 11,700 cal. year BP, an abrupt shift to lower χ_{lf} values indicates a quick and short duration return to a lake-level status similar to the LGM (low-amplitude oscillations and/or lake high-stand). Based on our independent chronology, this time interval then corresponds to the Younger Dryas event [YD: 12,800–11,600 cal. year BP (Bard and Kromer, 1995)].

The sharp ~11,700 cal. year BP transition corresponds to the boundary between Lithozone III and Lithozone IV, and is synchronous with the beginning of the Holocene. During the whole Holocene period, the χ_{lf} signal shows relatively high values and low variability, suggesting more stable environmental and climatic conditions than during glacial times. Holocene input of the MDTM fraction into the lake was probably associated with high-amplitude seasonal to decadal changes in lake level, which characterizes the present-day hydrological conditions of this area.

9. The spectral analysis of the χ_{lf} record and its climatic implications

To explore the origin of the Masoko depositional changes, we did a spectral analysis of the χ_{lf} record by using the REDFIT 3.5 software, which has the characteristic to work on unevenly spaced time series (Schulz and Mudelsee, 2002) and which allows one to estimate the significance level of spectral peaks relative to a red-noise spectrum (calculated by Monte Carlo, generating a large number of first order autoregressive processes). The resulting χ_{lf} spectrum (Fig. 9) shows that cyclic deposition at Lake Masoko occurred at multi-millennial, millennial, centennial and multi-decadal scales. This variability is marked by more than twelve spectral peaks exceeding the 90% limit of confidence, eight of them exceeding the 99% limit of confidence.

Three major peaks characterize the multi-millennial variability: respectively 22,660 years, 11,330 years and 7550 years. The 22,660-year period cannot be statistically inferred, because only two cycles were counted over the record. Nevertheless, these cycles are well observed with the naked eyes, suggesting a control of deposition (and inferred lake-level oscillations) by the ~23,000 years precessional cycle (Berger et al., 1993). The 11,330- and 7550-year spectral peaks correspond respectively to the half-precessional cycle (Berger and Loutre, 1997) and to a harmonic of the precession (Pokras and Mix, 1987). Together, these observations show that low frequency variability of deposition at Masoko is closely associated to the precession band, supporting a dominant forcing of low-latitude insolation on environmental and climate dynamics in tropical Africa (Thevenon et al., 2002; Trauth et al., 2003).

Due to the chronological limits of most radiocarbon-based age models in Late Quaternary sedimentary records, the identification of millennial and shorter cycles should be taken with caution and regarded as

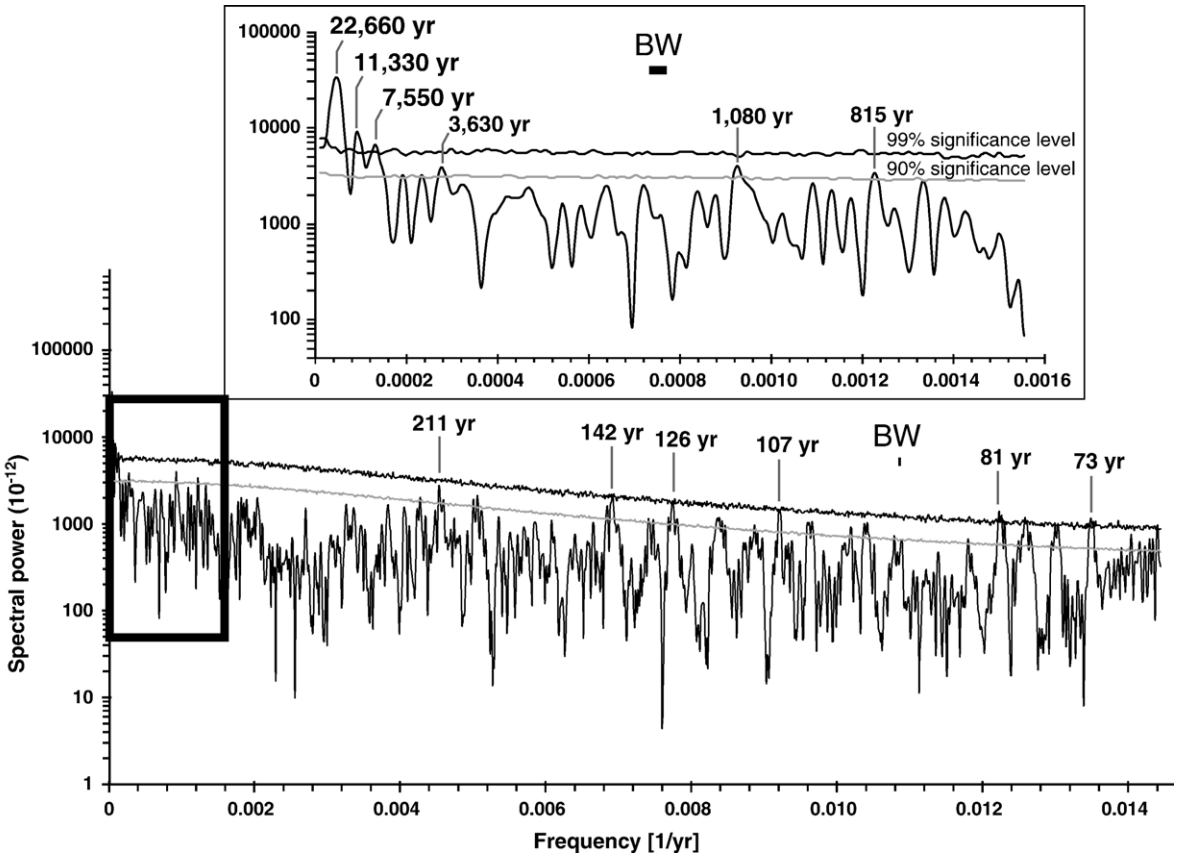

Fig. 9. Spectral analysis of the susceptibility record from Lake Masoko. Peaks are labelled with their period (in years). The spectral power (log scale) was calculated with REDFIT (Schulz and Mudelsee, 2002), using the Lomb-Scargle Fourier transform for unevenly spaced data, the Welch-overlapped-segment-averaging procedure (two segments with 50% overlap) and a rectangular window. 2000 Monte Carlo simulations were used for bias corrections of the red noise. The red noise spectra issued from a first-order autoregressive (AR1) process are shown as Monte Carlo upper bounds (90% and 99% significance levels in light gray and black, respectively). The 6-dB bandwidth (BW) determines the frequency resolution.

merely indicative. Three peaks dominate the millennial variability at Masoko, respectively 3630 years, 1080 years and 815 years, which exceed the 90% limit of confidence. A ~3300–4200-year cycle as been previously reported in several planktonic foraminifera $\delta^{18}O$ records from the South- and North-Tropical Indian Ocean (Pestiaux et al., 1988) and Arabian Sea (Sirocko et al., 1996), as well as in an East Asian Monsoon record from the Sulu Sea (de Garidel-Thoron et al., 2001). The origin of this cycle is unclear and possibly reflects combination tones of orbital parameters on monsoon dynamics (Pestiaux et al., 1988). At sub-millennial scale, higher frequency periodicities are generally poorly documented over long time intervals, most especially in low-latitude records. Nevertheless, strong variability in the ~990–1100-year, and 500–800-year bands has been reported in high latitude sites (Bond et al., 2001), in the Arabian Sea (Sirocko et al., 1996) and in the Late Holocene Makapansgat speleothem record of Southern Africa (Tyson et al., 2002). Although the occurrence of these cycles at Masoko is consistent with (i) the general control of the Indian and Pacific Ocean circulation on the hydrology of Eastern Africa and (ii) a connection between the high latitude climate variability and the climate of Southern Africa (Tyson et al., 2002), the persistence and robustness of such cycles as well as their global character over glacial–interglacial periods remains to be established.

In this way, neither the ~6000-year cycle nor the ~1500-year cycle, which characterize the North Atlantic climate and iceberg surges during glacial and post-glacial times (Dansgaard et al., 1993; Grootes et al., 1993; Schulz et al., 1999) as well as the East Asian winter monsoon proxies (de Garidel-Thoron et al., 2001; Thevenon et al., 2004), exceed the 90% limit of confidence in the Masoko record. This reinforces the idea that teleconnections between the south tropical hydrology and the millennial climate variability as

defined in the Northern Hemisphere might not be persistent over time (Schulz et al., 2004).

At a higher frequency, spectral peaks at 211 years and two other groups of peaks at 100–150 years (142, 126, 107 years) and 70–80 years (81, 73 years), most exceeding the 99% limit of confidence, characterize the highest frequency measurable with the resolution of our series. Spectral analysis as performed on shorter time windows (5000-year-long) indicates that these three spectral bands remain significant over the whole record. Such high-frequency variability has been detailed in (i) numerous high- and low-latitudinal Holocene environment and paleoclimatic records from both hemispheres (Anderson, 1992), (ii) atmospheric ^{14}C and ^{10}Be cosmogenic isotope production records from respectively tree-ring (Stuiver et al., 1991) and ice-cores (Beer et al., 1988), and (iii) historical records of sunspot number and solar activity (Ogurtsov et al., 2002). In addition, the latter correlate directly with the cosmogenic isotope production changes (Bard et al., 1997), summer temperature change in northern Europe (Ogurtsov et al., 2001), and lake level changes in Equatorial Africa (Verschuren et al., 2000; Stager et al., 2005).

For Southern Africa, a review of climate records from speleothems, tree-rings, and meteorological data (Tyson et al., 2002) shows intermittent 120–200-year cycles and persistent 60–120-year cycles. The 60–80-year cycles are observed in the Zambezi river discharge at Victoria Falls and in tree-ring records from the summer rainfall region, two proxies that display coherent and in-phase changes with the southern oscillation index (SOI) over the past decades.

As reported in such regions, a connection between solar activity and hydrology in the Rungwe south tropical region at decadal–centennial scale should not be excluded, considering that the 211-year peak could correspond to the Suess cycle (~200–250 years), while the 100–150-year and 70–80-year bands could correspond to the Gleissberg cycles (~110–140 years and ~80 years) (Ogurtsov et al., 2002).

10. Discussion

10.1. Depositional controls at Lake Masoko

Our results allow us to clarify the peculiar response of the Masoko basin to hydrological change. As evidenced from the very high hydraulic conductivity of soils and from the absence of rill erosion around the lake, the high porosity of the Masoko catchment precludes any direct and dominant control of sedimentary terrigenous inputs by surface runoff and rainfall. These observations imply a very limited control by runoff processes on the input of the MDTM component into the lake, therefore invalidating the preliminary interpretation of low sediment χ_{lf} values, associated to an arid period of reduced runoff and (Williamson et al., 1999). Instead, the peculiar geomorphological setting of the crater, coupled with the homogeneity of the catchment vegetation and geology, and the persistent oligotrophy of this freshwater lake (Barker et al., 2003), reinforces the importance of the shoreline area in the sedimentation processes. Indeed, lake level changes act on the MDTM supplier and in turn control the sediment χ_{lf}.

In view of the above results, a preliminary comparison with stable carbon isotopes (Gibert et al., 2002), lignin phenol (Merdaci, 1998) and diatom records (Barker et al., 2003) of cores M96-A and MM-8 does not support the former interpretation (Williamson et al., 1999; Barker et al., 2003) of lake low-stand period during the LGM at Lake Masoko. First, the lowest $\delta^{13}C$ values (less than −28‰ vs. PDB) of Total Organic Carbon (Gibert et al., 2002) and the maximum lignin phenol concentrations (Merdaci, 1998) observed between ~25,000 and ~15,000 cal. year BP, suggest the development of a C3 arboreal forest on the Masoko catchment during an arid LGM, in agreement with our inferred low seasonal hydrological variability and relatively humid climate. Second, the transfer function between diatom assemblages and water conductivity at Lake Masoko evidenced slightly higher water conductivities for the LGM period (~600 $\mu S\ cm^{-1}$) than during the Holocene (~400 $\mu S\ cm^{-1}$), while the ordination of diatom assemblages show an increase in benthic, shallow water diatoms for the LGM (Barker et al., 2003). We suggest that the inferred changes in water conductivity as well as the stronger inputs in benthic species during the LGM are probably constrained by other factors than evaporation and lake level. The development of the forest around the lake during the LGM likely resulted in a strengthened soil chemical weathering, supporting an increase in water conductivity. Moreover, the stabilization of the LGM lake level at seasonal to longer scales and the resulting enlargement of a perennial shallow water area could support a higher production of shallow water, light-demanding diatom species.

To be to be fully validated, our alternative interpretation of the Masoko hydrology during the last glacial period therefore needs further monitoring of the lake biogeochemistry as well as new climate proxy indicators (e.g., pollen, phytoliths and stable isotopes).

10.2. Comparison with other regional records

Due to the lack of detailed chronologies documenting continuous climatic changes in Africa for the last 45,000 years, the comparison between the LM record and other continental records from tropical Africa is restricted to the last 25,000–30,000 years at most. As previously suggested from the studies of cored sediments from Lake Tanganyika, Lake Victoria, Lake Malawi, Lake Rukwa and Lake Bosumtwi (Gasse et al., 1989; Johnson et al., 1996; Barker et al., 2002; Gasse et al., 2002; Peck et al., 2004), some major hydrological changes recorded at Lake Masoko appear synchronous with the high-latitude climate of the Northern Hemisphere (Fig. 10). This is especially the case for the LGM and YD time intervals, which correspond at Lake Masoko to wetter periods of low-amplitude lake-level oscillations and/or lake high-stand, indicating relatively humid conditions south of the Rungwe area. The sharp transition which characterizes the end of the YD event and the beginning of the Holocene in the North Atlantic (Taylor et al., 1997) is also well defined in the Masoko record, suggesting a major hydrological change in the southern ITCZ area.

One characteristic feature of the Masoko record is the strong centennial to millennial variability of deposition during the glacial period, which likely results from a connection between the low-latitude hydrological changes and the well-documented, high-latitude Dansgaard–Oeschger (D–O) climate variability of the North Atlantic area, paced by rapid iceberg discharges (Heinrich events) followed by abrupt warming (D–O interstadial phases) (Bond et al., 1992; Dansgaard et al., 1993) (Fig. 10). Owing to the high frequency of large

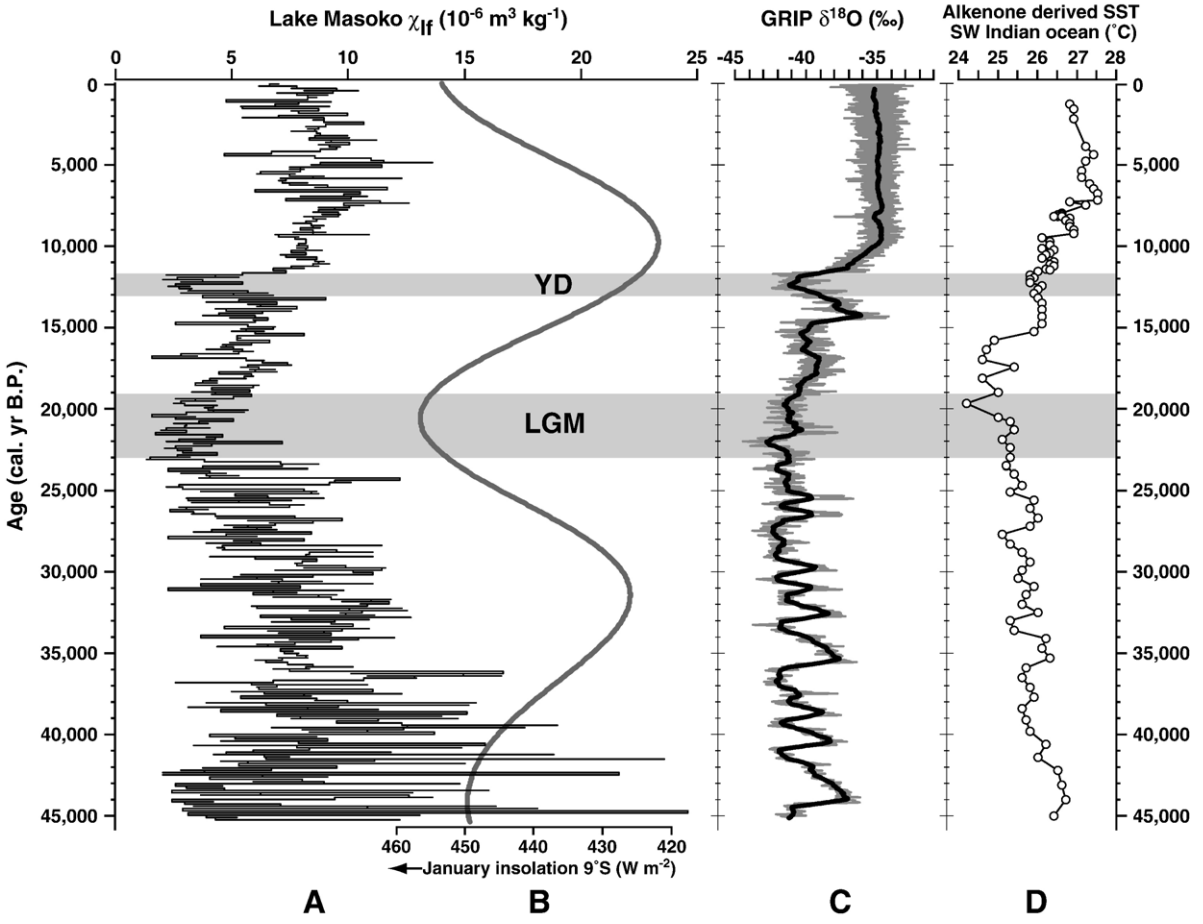

Fig. 10. Comparison of (A) the Lake Masoko magnetic susceptibility record (50-year averages) with (B) the January solar insolation for 9°S (Berger et al., 1993) (reversed scale), (C) the Greenland GRIP oxygen isotope record (Grootes et al., 1993) (black line shows 500-year averages; gray line shows 3-year averages) and (D) the alkenone-derived SST record from the Mozambique Channel, SW Indian Ocean (Sonzogni et al., 1998). The LGM and the YD intervals (black labels) are indicated by gray bands.

amplitude depositional changes recorded at Lake Masoko, a distinct identification of each individual D–O phase and Heinrich event is not straightforward. This suggests that the centennial to millennial hydrological variability in the Rungwe area was not exclusively connected to high latitude variability. Summertime insolation at 9°S is in phase with susceptibility maxima and minima (Fig. 10A and B), indicating that low-latitude insolation is a dominant forcing influence of the Masoko hydrological cycle.

A comparison of the Masoko record with other paleo-climatic and -hydrological records from the region reveals some strong local and regional contrasts. The nearest Sea Surface Temperature (SST) proxy record of the south-eastern Mozambique Channel (Sonzogni et al., 1998) indicates that the coolest SST time interval (20,000–15,500 cal. year BP) of the last glacial period lags the "LGM" time interval of Lake Masoko (23,000–19,000 cal. year BP) by ~2000 years (Fig. 10D).

Relatively wet conditions are inferred at Masoko during the LGM and the Younger Dryas event. This contrasts with most of the East African terrestrial records located to the north of our site (Gasse et al., 1989; Vincens et al., 1993; Johnson et al., 1996; Beuning et al., 1997; Bonnefille and Chalié, 2000; Gasse, 2000; Gasse et al., 2002), which indicate drier and cooler conditions during the LGM period and until 15,500 cal. year BP, the latter age corresponding to the beginning of the "lacustrine optimum" of intertropical Africa. Drier conditions are also evidenced in this region during the YD event (Roberts et al., 1993; Williamson et al., 1993; Beuning et al., 1997).

The apparent antiphasing between the hydrology of northern sites and Lake Masoko would support the hypothesis of a rapid southward shift of the ITCZ during the LGM and the YD event (Lea et al., 2003). To date, however, the most recent hydrological records from Lake Malawi, south of Masoko, do not support our inferred high-resolution hydrological changes.

In this lake, high-stand conditions have been previously reported for the LGM (Finney et al., 1996; Johnson, 1996). Based on recent organic geochemistry and diatom assemblages, proxy records of hydrological change, the Lake Malawi LGM interval is now reinterpreted as a dry, lake low-stand period (Gasse et al., 2002; Johnson et al., 2002; Filippi and Talbot, 2005), suggesting that the southern ITCZ area was drier during the LGM.

The Lake Masoko record therefore confirms that local and regional hydrological contrasts occurred in the ITCZ area during the last 45,000 years. Various causes could be invoked to explain an apparent antiphasing between the Masoko and Malawi hydrological changes. A strong control of regional (glacial) cooling (Powers et al., 2005) in the low altitude tropical (Rungwe) mountain ecosystems and local climates cannot be excluded, including a potential increase in rainfall over the Rungwe area associated with strengthened evaporation over Lake Malawi during the LGM dry season (Bergonzini, 1997).

Further local studies and regional synthesis of paleohydrological changes are consequently needed to better establish the extent of wetter (drier) conditions during glacial times in tropical Southern Africa.

11. Conclusion

The 45,000-year high-resolution Lake Masoko record provides insight into environmental and climatic changes in tropical Southern Africa across the late Pleistocene to Holocene. This long crater–lake record is characterized by a low mean sedimentation rate of ~0.33 mm year^{-1} and corresponds to a continuous deposition of lacustrine biogenic elements associated with terrigenous (clastic and organic) inputs from the catchment. Numerous turbidite and tephra layers are interbedded in the sediments. The resulting depositional record documents respectively the decreasing sensitivity of the crater slopes to gravity processes through time, and the persistent eruptive activity of the Rungwe volcanic centre since 45,000 years. Based on present-day observations and measurements, the low-field magnetic susceptibility of the sediment was used as a proxy of clastic terrigenous inputs enriched in coarse titanomagnetite, mostly originating from the shoreline sand reservoir. Erosional processes in the lake shore area are likely constrained by (i) the general lake status (low-stand or high-stand), which defines the distance between the lakeshore and the lake bottom, and (ii) the seasonal to interannual amplitude of lake-level changes associated with the severity of the dry "winter season", which define the storage efficiency of the sands in the shoreline area (low amplitude) or the delivery of these sands towards the deep lake (high amplitude).

The Masoko low-field susceptibility record for the last 45,000 years shows a general well-marked lake-level oscillations (seasonal to interannual) and/or low-stands. Two major time intervals show opposite trends: the Last Glacial Maximum and the Younger Dryas, where wetter conditions (stable lake and/or lake high-stand) are inferred. Although timing of these changes is synchronous with major global climatic changes, there is no direct relationship between the Lake Masoko and

other regional records from east tropical Africa, where lake low-stands and drier conditions during the LGM and the YD are generally inferred. Still, the Masoko record shows a strong variance in the precession and semi-precession bands, suggesting a low-latitude insolation forcing on the hydrology of the Rungwe highlands.

At centennial and millennial scales, the North Atlantic variability was partly identified at Lake Masoko, where wetter conditions prevailed during the YD, in agreement with (i) a southward shift of the ITCZ during stadial phases of the D–O variability (Lea et al., 2003) and/or (ii) a significant control of regional temperature changes (Powers et al., 2005) on the hydrology of the low altitude Rungwe mountain area.

The multi-decadal to centennial variability is relatively persistent over time and shows significant frequencies in the range of the Suess and Gleissberg solar cycles, indicating a probable forcing of solar activity on the Lake Masoko hydrological cycle, as observed for the recent past in other regional lacustrine records. Further work is needed to detail the coupled responses of terrestrial and aquatic ecosystem components to such hydrological changes in Africa.

Acknowledgments

Thanks are due to the ECC-RUKWA project team, which collected the cores in 1994 and 1996. A. Issah E. Mwandapile, S. Kajula, B. Gwambene, G. Buchet and M. Decobert are thanked for assisting us during fieldwork at Lake Masoko in 2003. We acknowledge the support of the Institute for Rock Magnetism (University of Minnesota) for inviting us to perform additional AC field dependent measurements of the magnetic susceptibility. O. Merdaci, L. Beaufort, J. Guiot, S. Brewer, and L. Bergonzini are warmly acknowledged for their scientific support during this study. We wish to thank M.R. Talbot and P. Barker for their encouragements to publish this work and M.A.J. Williams and an anonymous reviewer for their constructive comments. This research was supported by the CLEHA project of the ECLIPSE program (Institut National des Sciences de l'Univers), the RESOLVE project of the ACI Ecologie Quantitative program (Ministère Français de la Recherche), and the Tanzania Commission for Science and Technology (COSTECH).

References

Anderson, R.Y., 1992. Possible connection between surface winds, solar activity and the Earth's magnetic field. Nature 358, 51–54.

Avnimelech, Y., Ritvo, G., Meijer, L.E., Kochba, M., 2001. Water content, organic carbon and dry bulk density in flooded sediments. Aquacultural Engineering 25, 25–33.

Bard, E., Kromer, B., 1995. The Younger Dryas: absolute and radiocarbon chronology. In: Troelstra, S.R., van Hinte, J.E., Ganssen, G.M. (Eds.), The Younger Dryas. Proceedings of the Royal Dutch Academy of Science, pp. 161–166.

Bard, E., Raisbeck, G.M., Yiou, F., Jouzel, J., 1997. Solar modulation of cosmogenic nuclide production over the last millenium: comparison between ^{14}C and ^{10}Be records. Earth and Planetary Science Letters 150, 453–462.

Barker, P., Gasse, F., 2003. New evidence for a reduced water balance in East Africa during the Last Glacial Maximum: implication for model–data comparison. Quaternary Science Reviews 22, 823–837.

Barker, P., Telford, R., Merdaci, O., Williamson, D., Taieb, M., Vincens, A., Gibert, E., 2000. The sensitivity of a Tanzanian crater lake to catastrophic tephra input and four millennia of climate change. Holocene 10, 303–310.

Barker, P., Telford, R., Gasse, F., Thevenon, F., 2002. Late Pleistocene and Holocene palaeohydrology of Lake Rukwa, Tanzania, inferred from diatom analysis. Palaeogeography, Palaeoclimatology, Palaeoecology 187, 295–305.

Barker, P., Williamson, D., Gasse, F., Gibert, E., 2003. Climatic and volcanic forcing revealed in a 50,000-year diatom record from Lake Massoko, Tanzania. Quaternary Research 60, 368–376.

Beer, J., Siegenthaler, U., Bonani, G., Finkel, R.C., Oeschger, H., Suter, M., Wolfli, W., 1988. Information on past Solar-activity and geomagnetism from Be-10 in the camp century ice core. Nature 331, 675–679.

Berger, A., Loutre, M.F., 1997. Intertropical latitudes and precessional and half-precessional cycles. Science 278, 1476–1478.

Berger, A., Loutre, M.F., Tricot, C., 1993. Insolation and Earths orbital periods. Journal of Geophysical Research-Atmospheres 98, 10341–10362.

Bergonzini, L., 1997. Bilans hydriques de lacs du Rift Est-Africain (Kivu, Tanganyika, Rukwa et Nyassa). Approche mensuelle et annuelle. Essai d'interprétation de la variabilité inter-annuelle et des fluctuations passées. Unpublished Thesis, University Paris-Sud, Paris. 246 pp.

Bergonzini, L., Gibert, E., Winckel, A., Merdaci, O., 2001. Water and isotopic (O-18 and H-2) budget of Lake Massoko, Tanzania. Quantification of exchange between Lake and groundwater. Comptes Rendus de L'Académie des Sciences Serie: II. Fascicule a-Sciences de la Terre et des Planètes 333, 617–623.

Beuning, K.R.M., Talbot, M.R., Kelts, K., 1997. A revised 30,000-year paleoclimatic and paleohydrologic history of Lake Albert, East Africa. Palaeogeography, Palaeoclimatology, Palaeoecology 136, 259–279.

Bond, G., Heinrich, H., Broecker, W., Labeyrie, L., McManus, J., Andrews, J., Huon, S., Jantschik, R., Clasen, S., Simet, C., Tedesco, K., Klas, M., Bonani, G., Ivy, S., 1992. Evidence for massive discharges of icebergs into the North-Atlantic Ocean during the last glacial period. Nature 360, 245–249.

Bond, G., Kromer, B., Beer, J., Muscheler, R., Evans, M.N., Showers, W., Hoffmann, S., Lotti-Bond, R., Hajdas, I., Bonani, G., 2001. Persistent solar influence on North Atlantic climate during the Holocene. Science 294, 2130–2136.

Bonnefille, R., Chalié, F., 2000. Pollen-inferred precipitation time-series from equatorial mountains, Africa, the last 40 kyr BP. Global and Planetary Change 26, 25–50.

Brown, S., Bierman, P., Lini, A., Davis, P.T., Southon, J., 2002. Reconstructing lake and drainage basin history using terrestrial sediment layers: analysis of cores from a post-glacial lake in New England, USA. Journal of Paleolimnology 28, 219–236.

Dansgaard, W., Johnsen, S.J., Clausen, H.B., Dahljensen, D., Gundestrup, N.S., Hammer, C.U., Hvidberg, C.S., Steffensen, J. P., Sveinbjornsdottir, A.E., Jouzel, J., Bond, G., 1993. Evidence for general instability of past climate from a 250-kyr ice-core record. Nature 364, 218–220.

Day, R., Fuller, M., Schmidt, V.A., 1977. Hysteresis properties of titanomagnetites: grain size and compositional dependence. Earth and Planetary Science Letters 13, 260–267.

de Garidel-Thoron, T., Beaufort, L., Linsley, B.K., Dannenmann, S., 2001. Millennial-scale dynamics of the East Asian winter monsoon during the last 200,000 years. Paleoceanography 16, 491–502.

de Wall, H., 2000. The field-dependence of AC susceptibility in titanomagnetites: implications for the anisotropy of magnetic susceptibility. Geophysical Research Letters 27, 2409–2411.

Delvaux, D., Khan, M.A., 1998. Tectonics, sedimentation and volcanism in the East African Rift System: introduction. Journal of African Earth Sciences 26, 343–346.

Dupre, B., Dessert, C., Oliva, P., Godderis, Y., Viers, J., Francois, L., Millot, R., Gaillardet, J., 2003. Rivers, chemical weathering and Earth's climate. Comptes Rendus Geosciences 335, 1141–1160.

Ebinger, C.J., Deino, A.L., Drake, R.E., Tesha, A.L., 1989. Chronology of volcanism and rift basin propagation – Rungwe Volcanic Province, East-Africa. Journal of Geophysical Research–Solid Earth and Planets 94, 15785–15803.

Ebinger, C.J., Deino, A.L., Tesha, A.L., Becker, T., Ring, U., 1993. Tectonic controls on rift basin morphology – evolution of the Northern Malawi (Nyasa) Rift. Journal of Geophysical Research–Solid Earth 98, 17821–17836.

Eden, D.N., Page, M.J., 1998. Palaeoclimatic implications of a storm erosion record from late Holocene lake sediments, North Island, New Zealand. Palaeogeography, Palaeoclimatology, Palaeoecology 139, 37–58.

Ficken, K.J., Street-Perrott, F.A., Perrott, R.A., Swain, D.L., Olago, D. O., Eglinton, G., 1998. Glacial/interglacial variations in carbon cycling revealed by molecular and isotope stratigraphy of Lake Nkunga, Mt. Kenya, East Africa. Organic Geochemistry 29, 1701–1719.

Ficken, K.J., Wooller, M.J., Swain, D.L., Street-Perrott, F.A., Eglinton, G., 2002. Reconstruction of a subalpine grass-dominated ecosystem, Lake Rutundu, Mount Kenya: a novel multi-proxy approach. Palaeogeography, Palaeoclimatology, Palaeoecology 177, 137–149.

Filippi, M.L., Talbot, M.R., 2005. The palaeolimnology of northern Lake Malawi over the last 25 ka based upon the elemental and stable isotopic composition of sedimentary organic matter. Quaternary Science Reviews 24, 1303–1328.

Finney, B.P., Scholz, C.A., Johnson, T.C., Trumbore, S., 1996. Late Quaternary lake-level changes of Lake Malawi. In: Johnson, T.C., Odada, E.O. (Eds.), The Limnology, Climatology and Paleoclimatology of the East African Lakes. Gordon and Breach Publishers, Amsterdam, pp. 495–508.

Gasse, F., 2000. Hydrological changes in the African tropics since the Last Glacial Maximum. Quaternary Science Reviews 19, 189–211.

Gasse, F., Ledee, V., Massault, M., Fontes, J.C., 1989. Water-level fluctuations of Lake Tanganyika in phase with oceanic changes during the last glaciation and deglaciation. Nature 342, 57–59.

Gasse, F., Barker, P., Johnson, T., 2002. A 24,000 yr diatom record from the northern basin of Lake Malawi. In: Odada, E.O., Olago, D.O. (Eds.), The East African Great Lakes: Limnology, Palaeolimnology and Biodiversity. Kluwer Academic Publishers, Dordrecht, Netherlands, pp. 393–414.

Gibert, E., Bergonzini, L., Massault, M., Williamson, D., 2002. AMS-C-14 chronology of 40.0 cal ka BP continuous deposits from a crater lake (Lake Massoko, Tanzania) – modern water balance and environmental implications. Palaeogeography, Palaeoclimatology, Palaeoecology 187, 307–322.

Grootes, P.M., Stuiver, M., White, J.W.C., Johnsen, S., Jouzel, J., 1993. Comparison of oxygen-isotope records from the GISP2 and GRIP Greenland ice cores. Nature 366, 552–554.

Harkin, D.A., 1960. The Rungwe volcanics at the northern end of Lake Nyasa. Geologic Survey of Tanganyika, Dodoma, pp. 172.

Huang, Y.S., Street-Perrott, F.A., Perrot, R.A., Metzger, P., Eglinton, G., 1999. Glacial–interglacial environmental changes inferred from molecular and compound-specific delta C-13 analyses of sediments from Sacred Lake, Mt. Kenya. Geochimica et Cosmochimica Acta 63, 1383–1404.

Jackson, M., Moskowitz, B., Rosenbaum, J., Kissel, C., 1998. Field-dependence of AC susceptibility in titanomagnetites. Earth and Planetary Science Letters 157, 129–139.

Johnson, T.C., 1996. Sedimentary processes and signals of past climatic change in the large lakes of the East African rift valley. In: Johnson, T.C., Odada, E.O. (Eds.), The Limnology, Climatology and Paleoclimatology of the East African Lakes. Gordon and Breach Publishers, Amsterdam, pp. 367–412.

Johnson, T.C., Scholz, C.A., Talbot, M.R., Kelts, K., Ricketts, R.D., Ngobi, G., Beuning, K., Ssemmanda, I., McGill, J.W., 1996. Late Pleistocene desiccation of Lake Victoria and rapid evolution of cichlid fishes. Science 273, 1091–1093.

Johnson, T.C., Brown, E.T., McManus, J., Barry, S., Barker, P., Gasse, F., 2002. A high-resolution paleoclimate record spanning the past 25,000 years in southern East Africa. Science 296, 113–132.

Lea, D.W., Pak, D.K., Peterson, L.C., Hughen, K.A., 2003. Synchroneity of tropical and high-latitude Atlantic temperatures over the Last Glacial Termination. Science 301, 1361–1364.

Maley, J., Brenac, P., 1998. Vegetation dynamics, palaeoenvironments and climatic changes in the forests of western Cameroon during the last 28,000 years BP. Review of Palaeobotany and Palynology 99, 157–187.

Mayewski, P.A., Rohling, E.E., Stager, J.C., Karlen, W., Maasch, K. A., Meeker, L.D., Meyerson, E.A., Gasse, F., van Kreveld, S., Holmgren, K., Lee-Thorp, J., Rosqvist, G., Rack, F., Staubwasser, M., Schneider, R.R., Steig, E.J., 2004. Holocene climate variability. Quaternary Research 62, 243–255.

Merdaci, O., 1998. Changements climatiques au cours des derniers 30 000 ans en Afrique Sud-Equatoriale (Tanzanie) par l'étude des pigments et phénols lacustres. Unpublished Thesis, University Aix-Marseille III. 208 pp.

Millot, R., Gaillardet, J., Dupre, B., Allegre, C.J., 2002. The global control of silicate weathering rates and the coupling with physical erosion: new insights from rivers of the Canadian Shield. Earth and Planetary Science Letters 196, 83–98.

Mix, A.C., Bard, E., Schneider, R., 2001. Environmental processes of the ice age: land, oceans, glaciers (EPILOG). Quaternary Science Reviews 20, 627–657.

Morgan, V., Delmotte, M., van Ommen, T., Jouzel, J., Chappellaz, J., Woon, S., Masson-Delmotte, V., Raynaud, D., 2002. Relative timing of deglacial climate events in Antarctica and Greenland. Science 297, 1862–1864.

New, M., Lister, D., Hulme, M., Makin, I., 2002. A high-resolution data set of surface climate over global land areas. Climate Research 21, 1–25.

Nicholson, S.E., 1986. The nature of rainfall variability in Africa south of the equator. Journal of Climatology 6, 515–530.

Nicholson, S., Yin, X., 2002. Mesoscale patterns of rainfall, cloudiness and evaporation over the Great Lakes of Africa. In: Odada, E.O., Olago, D.O. (Eds.), The East African Great Lakes: Limnology, Palaeolimnology and Biodiversity. Kluwer Academic Publishers, Dordrecht, Netherlands, pp. 93–120.

Ogurtsov, M.G., Kocharov, G.E., Lindholm, M., Eronen, M., Nagovitsyn, Y.A., 2001. Solar activity and regional climate. Radiocarbon 43, 439–447.

Ogurtsov, M.G., Kocharov, G.E., Lindholm, M., Merilainen, J., Eronen, M., Nagovitsyn, Y.A., 2002. Evidence of solar variation in tree-ring-based climate reconstructions. Solar Physics 205, 403–417.

Page, M.J., Trustrum, N.A., Dymond, J.R., 1994. Sediment budget to assess the geomorphic effect of a cyclonic storm, New-Zealand. Geomorphology 9, 169–188.

Peck, J.A., Green, R.R., Shanahan, T., King, J.W., Overpeck, J.T., Scholz, C.A., 2004. A magnetic mineral record of Late Quaternary tropical climate variability from Lake Bosumtwi, Ghana. Palaeogeography, Palaeoclimatology, Palaeoecology 215, 37–57.

Pestiaux, P., van der Mersch, I., Berger, A., Duplessy, J.C., 1988. Paleoclimatic variability at frequencies ranging from 1 cycle per 10000 years to 1 cycle per 1000 years: evidence for nonlinear behaviour of the climate system. Climatic Change 12, 9–37.

Peterson, L.C., Haug, G.H., Hughen, K.A., Rohl, U., 2000. Rapid changes in the hydrologic cycle of the tropical Atlantic during the last glacial. Science 290, 1947–1951.

Pierce, L.R., 2004. Lake waves, coarse clastic beach variability and management implications, Loch Lomond, Scotland, UK. Journal of Coastal Research 20, 562–585.

Pinot, S., Ramstein, G., Harrison, S.P., Prentice, I.C., Guiot, J., Stute, M., Joussaume, S., 1999. Tropical paleoclimates at the Last Glacial Maximum: comparison of Paleoclimate Modeling Intercomparison Project (PMIP) simulations and paleodata. Climate Dynamics 15, 857–874.

Pokras, E.M., Mix, A.C., 1987. Earths precession cycle and Quaternary climatic-change in tropical Africa. Nature 326, 486–487.

Powers, L.A., Johnson, T.C., Werne, J.P., Castanada, I.S., Hopmans, E.C., Damste, J.S.S., Schouten, S., 2005. Large temperature variability in the southern African tropics since the Last Glacial Maximum. Geophysical Research Letters 32, L08706, doi:10.1029/2004GL022014.

Rahmstorf, S., 2003. Timing of abrupt climate change: a precise clock. Geophysical Research Letters 30, 1510, doi:10.1029/2003GL017115.

Roberts, N., Taieb, M., Barker, P., Damnati, B., Icole, M., Williamson, D., 1993. Timing of the Younger Dryas Event in East-Africa from lake-level changes. Nature 366, 146–148.

Schulz, M., Mudelsee, M., 2002. REDFIT: estimating red-noise spectra directly from unevenly spaced paleoclimatic time series. Computers and Geosciences 28, 421–426.

Schulz, M., Berger, W.H., Sarnthein, M., Grootes, P.M., 1999. Amplitude variations of 1470-year climate oscillations during the last 100,000 years linked to fluctuations of continental ice mass. Geophysical Research Letters 26, 3385–3388.

Schulz, M., Paul, A., Timmermann, A., 2004. Glacial–interglacial contrast in climate variability at centennial-to-millennial time-scales: observations and conceptual model. Quaternary Science Reviews 23, 2219–2230.

Sirocko, F., GarbeSchonberg, D., McIntyre, A., Molfino, B., 1996. Teleconnections between the subtropical monsoons and high-latitude climates during the last deglaciation. Science 272, 526–529.

Sonzogni, C., Bard, E., Rostek, F., 1998. Tropical sea-surface temperatures during the last glacial period: a view based on alkenones in Indian Ocean sediments. Quaternary Science Reviews 17, 1185–1201.

Stager, J.C., Ryves, D., Cumming, B.F., Meeker, L.D., Beer, J., 2005. Solar variability and the levels of Lake Victoria, East Africa, during the last millenium. Journal of Paleolimnology 33, 243–251.

Street, F.A., Grove, A.T., 1979. Global maps of lake-level fluctuations since 30,000 yr B.P. Quaternary Research 12, 83–118.

Stuiver, M., Braziunas, T.F., Becker, B., Kromer, B., 1991. Climatic, solar, oceanic, and geomagnetic influences on late-glacial and Holocene atmospheric $^{14}C/^{12}C$ change. Quaternary Research 35, 1–24.

Talbot, M.R., Johannessen, T., 1992. A high-resolution paleoclimatic record for the last 27,500 years in tropical west Africa from the carbon and nitrogen isotopic composition of lacustrine organic-matter. Earth and Planetary Science Letters 110, 23–37.

Taylor, K.C., Mayewski, P.A., Alley, R.B., Brook, E.J., Gow, A.J., Grootes, P.M., Meese, D.A., Saltzman, E.S., Severinghaus, J.P., Twickler, M.S., White, J.W.C., Whitlow, S., Zielinski, G.A., 1997. The Holocene Younger Dryas transition recorded at Summit, Greenland. Science 278, 825–827.

Thevenon, F., Williamson, D., Taieb, M., 2002. A 22 kyr BP sedimentological record of Lake Rukwa (8°S, S–W Tanzania): environmental, chronostratigraphic and climatic implications. Palaeogeography, Palaeoclimatology, Palaeoecology 187, 285–294.

Thevenon, F., Williamson, D., Vincens, A., Taieb, M., Merdaci, O., Decobert, M., Buchet, G., 2003. A late-Holocene charcoal record from Lake Masoko, SW Tanzania: climatic and anthropologic implications. Holocene 13, 785–792.

Thevenon, F., Bard, E., Williamson, D., Beaufort, L., 2004. A biomass burning record from the West Equatorial Pacific over the last 360 ky: methodological, climatic and anthropic implications. Palaeogeography, Palaeoclimatology, Palaeoecology 213, 83–99.

Thouveny, N., Williamson, D., 1988. Paleomagnetic study of the Holocene and Upper Pleistocene sediments from Lake Barombi Mbo, Cameroun – 1st results. Physics of the Earth and Planetary Interiors 52, 193–206.

Thouveny, N., Debeaulieu, J.L., Bonifay, E., Creer, K.M., Guiot, J., Icole, M., Johnsen, S., Jouzel, J., Reille, M., Williams, T., Williamson, D., 1994. Climate variations in Europe over the past 140-kyr deduced from rock magnetism. Nature 371, 503–506.

Trauth, M.H., Deino, A.L., Bergner, A.G.N., Strecker, M.R., 2003. East African climate change and orbital forcing during the last 175 kyr BP. Earth and Planetary Science Letters 206, 297–313.

Tyson, P.D., Cooper, G.R.J., McCarthy, T.S., 2002. Millennial to multi-decadal variability in the climate of southern Africa. International Journal of Climatology 22, 1105–1117.

Verschuren, D., Laird, K.R., Cumming, B.F., 2000. Rainfall and drought in equatorial east Africa during the past 1,100 years. Nature 403, 410–414.

Vincens, A., Chalie, F., Bonnefille, R., Guiot, J., Tiercelin, J.-J., 1993. Pollen-derived rainfall and temperature estimates from Lake Tanganyika and their implication for Late Pleistocene water levels. Quaternary Research 40, 343–350.

Vincens, A., Williamson, D., Thevenon, F., Taieb, M., Buchet, G., Decobert, M., Thouveny, N., 2003. Pollen-based vegetation changes in southern Tanzania during the last 4200 years: climate change and/or human impact. Palaeogeography, Palaeoclimatology, Palaeoecology 198, 321–334.

Wang, Y.J., Cheng, H., Edwards, R.L., An, Z.S., Wu, J.Y., Shen, C.C., Dorale, J.A., 2001. A high-resolution absolute-dated Late Pleistocene monsoon record from Hulu Cave. China. Science 294, 2345–2348.

White, F., 1983. The Vegetation of Africa. A descriptive Memoir to Accompagny the UNESCO/AETFAT/UNSO Vegetation Map of Africa. In: UNESCO (Ed.), Paris, p. 356.

Williams, T.M., Henney, P.J., Owen, R.B., 1993. Recent eruptive episodes of the Rungwe volcanic field (Tanzania) recorded in lacustrine sediments of the Northern Malawi Rift. Journal of African Earth Sciences 17, 33–39.

Williamson, D., Taieb, M., Damnati, B., Icole, M., Thouveny, N., 1993. Equatorial extension of the Younger Dryas event: rock-magnetic evidence from Lake Magadi. Global and Planetary Change 7, 235–242.

Williamson, D., Jackson, M.J., Banerjee, S.K., Marvin, J., Merdaci, O., Thouveny, N., Decobert, M., Gibert-Massault, E., Massault, M., Mazaudier, D., Taieb, M., 1999. Magnetic signatures of hydrological change in a tropical maar-lake (Lake Massoko, Tanzania): preliminary results. Physics and Chemistry of the Earth. Part a–Solid Earth and Geodesy 24, 799–803.

Wilmshurst, J.M., McGlone, M.S., Partridge, T.R., 1997. A late Holocene history of natural disturbance in lowland podocarp/hardwood forest, Hawke's Bay, New Zealand. New Zealand Journal of Botany 35, 79–96.